NUCL SCI TECH (2017) 28:76
DOI 10.1007/s41365-017-0234-7

Impact of photoneutrons on reactivity measurements for TMSR-SF1

Rui-Min Ji[1,2] · Ming-Hai Li[1] · Yang Zou[1] · Gui-Min Liu[1]

Received: 16 July 2016 / Revised: 11 October 2016 / Accepted: 16 October 2016 / Published online: 28 April 2017

Abstract The solid-fueled thorium molten salt reactor (TMSR-SF1) is a 10 MW_{th} test reactor design to be deployed in 5–10 years by the TMSR group. Its design combines coated particle fuel and molten FLiBe coolant for great intrinsic safety features and economic advantages. Due to a large amount of beryllium in the coolant salt, photoneutrons are produced by (γ, n) reaction, hence the increasing fraction of effective delayed neutrons in the core by the photoneutrons originating from the long-lived fission products. Some of the delayed photoneutron groups are of long lifetime, so a direct effect is resulted in the transient process and reactivity measurement. To study the impact of photoneutrons for TMSR-SF1, the effective photoneutron fraction is estimated using k-ratio method and performed by the Monte Carlo code (MCNP5) with ENDF/B-VII cross sections. Based on the coupled neutron–photon point kinetics equations, influence of the photoneutrons is analyzed. The results show that the impact of photoneutrons is not negligible in reactivity measurement. Without considering photoneutrons in on-line reactivity measurement based on inverse point kinetics can result in overestimation of the positive reactivity and underestimation of the negative reactivity. The photoneutrons also lead to more waiting time for the doubling time measurement. Since the photoneutron precursors take extremely long time to achieve equilibrium, a "steady" power operation may not directly imply a "real" criticality.

Keywords TMSR-SF1 · Delayed photoneutrons · Coupled neutron–photon point kinetics · Reactivity measurement

This work was supported by the "Strategic Priority Research Program" of the Chinese Academy of Sciences (No. XDA02010000) and the Frontier Science Key Program of the Chinese Academy of Sciences (No. QYZDY-SSW-JSC016).

✉ Yang Zou
zouyang@sinap.ac.cn

✉ Gui-Min Liu
liuguimin@sinap.ac.cn

1 Shanghai Institute of Applied Physics, Chinese Academy of Sciences, Jiading Campus, Shanghai 201800, China

2 University of Chinese Academy of Sciences, Beijing 100049, China

1 Introduction

In recent years, fluoride-cooled high-temperature reactors (FHRs) have gained much attention worldwide due to the potential of achieving outstanding economic performance while meeting high standards for reactor safety and security [1–3]. With superior nuclear properties and heat-transfer characteristics, the FLiBe salt (LiF–BeF_2) becomes the most convincing medium for FHRs with thermal neutron spectrum [4]. The thorium molten salt reactor (TMSR) group in China proposed its research program [5, 6] including a 10 MW_{th} solid-fueled thorium molten salt reactor (TMSR-SF1). In this design, about 15,000 pebbles are loaded in the core cavity and about 5 m^3 FLiBe salt are filled in the primary loop.

Because of the large amount of beryllium in the core, photoneutrons are generated in the active region via (γ, n) reaction. In general, photoneutrons have little contributions to the overall neutron balance. They affect reactor power level in a negligible manner. However, there are some photoneutrons that are indirectly generated from fission, hence the term of delayed neutrons. Since photoneutrons have insignificant contribution to the fraction of effective delayed neutron and the equilibrium state is difficult to reach, the photoneutrons are often neglected, which results in measurement errors [7–12]. In VVRSZM type research reactor of KFKI-AEKI [10], which uses beryllium reflector, the reactivity meter gave false values because the photoneutrons were not taken into account. In HW-1, a uranium-fueled and heavy water moderated reactor built in China, it is observed that the critical water level is different at different power levels. In the rod-drop measurement on the LITR reactor of beryllium reflector, an underestimation of 6% was seen in the results by neglecting the photoneutrons [12].

In this paper, the impact of photoneutrons on reactivity measurement for TMSR-SF1 is investigated using neutron–photon coupled point kinetic equations. The methods are introduced in Sect. 2. The results are presented in Sect. 3. The conclusions are given in Sect. 4.

2 Methods

2.1 The *k*-ratio method

In 1997, Bretscher of the Argonne National Laboratory introduced the *k*-ratio method to evaluate the delayed neutron fraction [13]. According to this method, the fraction of effective delayed neutron can be evaluated by the ratio between the prompt and the total multiplication factors, hence the name of *k*-ratio method,

$$\begin{aligned}\beta_{\mathrm{eff}} &= \frac{\langle \chi_{\mathrm{d}} \upsilon_{\mathrm{d}} \rangle}{\langle \chi \upsilon \rangle} = 1 - \frac{\langle \chi \upsilon - \chi_{\mathrm{d}} \upsilon_{\mathrm{d}} \rangle}{\langle \chi \upsilon \rangle} = 1 - \frac{\langle \chi \upsilon_{\mathrm{p}} - (\chi_{\mathrm{d}} - \chi) \upsilon_{\mathrm{d}} \rangle}{\langle \chi \upsilon \rangle} \\ &\approx 1 - \frac{\langle \chi_{\mathrm{p}} \upsilon_{\mathrm{p}} \rangle}{\langle \chi \upsilon \rangle} = 1 - \frac{k_{\mathrm{p}}}{k},\end{aligned} \tag{1}$$

where υ, υ_{d} and υ_{p} are average numbers of the total fission neutrons, delayed fission neutrons and prompt fission neutrons, respectively, produced per fission; χ, χ_{d} and χ_{p} are spectra of the three neutron categories, respectively. The approximation in Eq. (1) is based on two assumptions: (1) $(\chi_{\mathrm{d}} - \chi)\upsilon_{\mathrm{d}}$ is at least two orders of magnitude smaller than the $\chi\upsilon_{\mathrm{p}}$, because υ_{d} is two orders of magnitude smaller than υ_{p}; and (2) χ_{p} is almost equal to χ.

The *k*-ratio method can be performed by Monte Carlo code (MCNP) which can suppress the delayed neutrons in the critical calculation. In this paper, MCNP5 (ver1.51) and ENDF/B-VII are used. The fraction of effective delayed fission neutrons (β^{n}), which are decayed by the fission products, is modeled by MCNP calculation (MODE N) with and without the delayed neutron (TOTNU card), while ignoring photoneutrons. β^{n} can be estimated by Eq. (2)

$$\beta^{\mathrm{n}} = \frac{k_{\mathrm{t}}^{\mathrm{n}} - k_{\mathrm{p}}^{\mathrm{n}}}{k_{\mathrm{t}}^{\mathrm{n}}}, \tag{2}$$

where the superscript n stands for MODE N, the subscript t and p denote the neutron transportation with and without the delayed neutron, respectively. As an extension, the contribution of photoneutrons (β^{ph}) can be obtained by coupled neutron–photon transport (MODE N P) with MPN card to model (γ, n) reaction [8],

$$\beta^{\mathrm{ph}} = \beta^{\mathrm{total}} - \beta^{\mathrm{n}} = \frac{k_{\mathrm{t}}^{\mathrm{n+p}} - k_{\mathrm{p}}^{\mathrm{n}}}{k_{\mathrm{t}}^{\mathrm{n+p}}} - \frac{k_{\mathrm{t}}^{\mathrm{n}} - k_{\mathrm{p}}^{\mathrm{n}}}{k_{\mathrm{t}}^{\mathrm{n}}}, \tag{3}$$

where the superscript n + p stands for MODE N P.

There is an approximation in the simulation. Because MCNP does not simulate the delayed particles in critical calculations, the prompt gammas emitted in the process of fission and neutron capture are used, instead of delayed gammas which are emitted in the decay process of the fission products and activation products. It is reasonable, as the difference is small between the prompt and delayed photon spectra from ^{235}U fission represented by empirical Eqs. (4) and (5) [8, 14].

$$\chi_{\mathrm{p}}^{\gamma}(E)v_{\mathrm{p}}^{\gamma}[\text{photons} \times \text{fission}^{-1} \times \text{MeV}^{-1}] = 8.0\exp(-1.1\,\mathrm{E}), \tag{4}$$

$$\chi_{\mathrm{d}}^{\gamma}(E)v_{\mathrm{d}}^{\gamma}[\text{photons} \times \text{fission}^{-1} \times \text{MeV}^{-1}] = 7.4 exp(-1.1\,\mathrm{E}). \tag{5}$$

2.2 The neutron–photon coupled point kinetics equations

With the infinite-velocity approximation, we can get the conventional set of point kinetics equations as Eqs. (6–8). The physical interpretation of this approximation is that the photons are transported instantaneously following a change. This approach has been used for fast neutrons in the neutron-only multi-group transportation [14]. Since the speed of photons is at least one order of magnitude greater than the neutron speed, it is more reasonable here.

$$\frac{\mathrm{d}n(t)}{\mathrm{d}t} = \frac{\rho * - \beta_{\mathrm{eff}}}{\Lambda^{\mathrm{n}}} n(t) + \sum_i \lambda_i C_i + \sum_j \lambda_j C_j, \tag{6}$$

$$\frac{dC_i(t)}{\mathrm{d}t} = \frac{\beta_i^n}{\Lambda^n} n(t) - \lambda_{ii}, \tag{7}$$

$$\frac{\mathrm{d}C_j(t)}{\mathrm{d}t} = \frac{\beta_j^{\mathrm{ph}}}{\Lambda^{\mathrm{n}}} n(t) - \lambda_j C_j, \tag{8}$$

where $n(t)$ is neutron flux (or power), C_i is concentration of the ith group of neutron precursors, λ_i is decay constant of the ith neutron precursors, $C_j = \rho^{\mathrm{ph}}\Lambda^{\gamma}/(\Lambda^{\mathrm{n}}P_j)$ is concentration of the ^{j}th group artificially introduced photoneutron precursors, ρ^{ph} is the photoneutrons reactivity (photoneutron production rate over photo removal rate), P_j is concentration of the jth group photoneutron precursors, λ_j is decay constant of the jth photoneutron precursor. Λ^{n} is neutron generation time, $\rho^* \equiv \rho + \rho^{\mathrm{ph}}$ is the total reactivity, $\beta_{\mathrm{eff}} = \sum_i \beta_i^{\mathrm{n}} + \sum_j \beta_j^{\mathrm{ph}}$ is the total effective delayed neutron fraction, β_i^{n} is the ith group delayed fission neutron fraction, β_j^{ph} is effective fraction of the jth group delayed photoneutrons, and Λ^{γ} is photon generation time.

The coefficients of β_{eff} and Λ^{n} are assumed to be independent of time. This is already the case for the exact point kinetic without photoneutron terms. The photoneutron reactivity is contributed by the gamma ray (both prompt and delayed) reactivity. Also, it is no need to calculate the photon generation time (Λ^{γ}) and the photoneutron precursor's concentration (P_j) to get the artificial photoneutron precursor group C_j for the dynamic behavior of the reactor [14].

As listed Table 1, the traditional 6 group delayed fission neutrons parameters per ^{235}U fission [15], and the additional 9 group delayed photoneutrons parameters per ^{235}U fission in infinite beryllium, are used together with the corrected effective fraction of the photoneutrons.

2.3 Interpretation of reactivity measurements

Because of the photoneutrons in the core, the in-hour equation used to convert a measured stable doubling period T into a reactivity ρ should be modified as Eq. (9) [10].

$$\frac{\rho(\$)}{\beta_{\mathrm{eff}}} = \frac{0.693\Lambda^{\mathrm{n}}}{T} + \sum\nolimits_i \frac{\beta_i^{\mathrm{n}}}{1+\frac{T\lambda_i}{0.693}} + \sum\nolimits_j \frac{\beta_j^{\mathrm{ph}}}{1+\frac{T\lambda_j}{0.693}}. \tag{9}$$

Similarly, for the interpretation of inverse kinetics measurements, the time-dependent reactivity $\rho(t)$ obtained by the evolution of the neutron population are modified as Eq. (10) [16, 17].

Table 1 Traditional delayed fission neutron parameters and additional photoneutron parameters [15]

Delayed neutrons			Delayed photoneutrons		
i	$\lambda_i \times (\mathrm{s}^{-1})$	$\beta_i\ (\times 10^{-4})$	j	$\lambda_j \times (\mathrm{s}^{-1})$	$\beta_j\ (\times 10^{-5})$
1	0.0124	2.47	1	6.24×10^{-7}	0.057
2	0.0305	13.85	2	2.48×10^{-6}	0.038
3	0.111	12.22	3	1.59×10^{-5}	0.260
4	0.311	26.45	4	6.20×10^{-5}	3.2
5	1.14	8.32	5	2.67×10^{-4}	0.36
6	3.01	1.69	6	7.42×10^{-4}	3.68
			7	$3.60 \times 10^{-}$	1.85
			8	8.85×10^{-3}	3.66
			9	2.26×10^{-2}	2.07

$$\begin{aligned}\frac{\rho(t)}{\beta_{\mathrm{eff}}} = 1 &+ \frac{\Lambda^{\mathrm{n}}}{\beta_{\mathrm{eff}} n(t)}\frac{\mathrm{d}n(t)}{\mathrm{d}t} - \frac{\Lambda^{\mathrm{n}}}{\beta_{\mathrm{eff}} n(t)}\sum_{i=1}^{6}\lambda_i C_i^0 BF_i \mathrm{e}^{-\lambda_i t} \\ &- \frac{1}{\beta_{\mathrm{eff}} n(t)}\int_0^t n(t')\sum_{i=1}^{6}\lambda_i\beta_i e^{-\lambda_i(t-t')}\mathrm{d}t' - \frac{\Lambda^{\mathrm{n}}}{\beta_{\mathrm{eff}} n(t)}\sum_{j=1}^{9}\lambda_j C_j^0 BF_j e^{-\lambda_j t} \\ &- \frac{1}{\beta_{\mathrm{eff}} n(t)}\int_0^t n(t')\sum_{j=1}^{9}\lambda_j\beta_j e^{-\lambda_j(t-t')}\mathrm{d}t',\end{aligned} \tag{10}$$

where C_j^0 and C_i^0 are the equilibrium concentration of neutron and photoneutron precursors, respectively; BF_i and BF_j are the build-up factors which account for the building up of delayed neutron and photoneutron precursors, respectively, prior to the actual measurement. The building factors can be derived from the power history before the measurement *via* Eq. (11), where, n_0 is the neutron flux at full power and T_{b} is the building up time.

$$BF_i = \lambda_i \int_{-T_{\mathrm{b}}}^{0} \frac{n(t)}{n_0} e^{\lambda_i t'}\mathrm{d}t'. \tag{11}$$

3 Results

MCNP5 is used for explicitly representing the geometry of TMSR-SF1, as shown schematically in Fig. 1. The graphite reflectors build up the core cavity and host the control rods and instruments. Fuel pebbles of Φ6 cm are filled in the core cavity and cooled by the FLiBe salt. Details of TMSR-SF1 can be found in Refs. [6, 19].

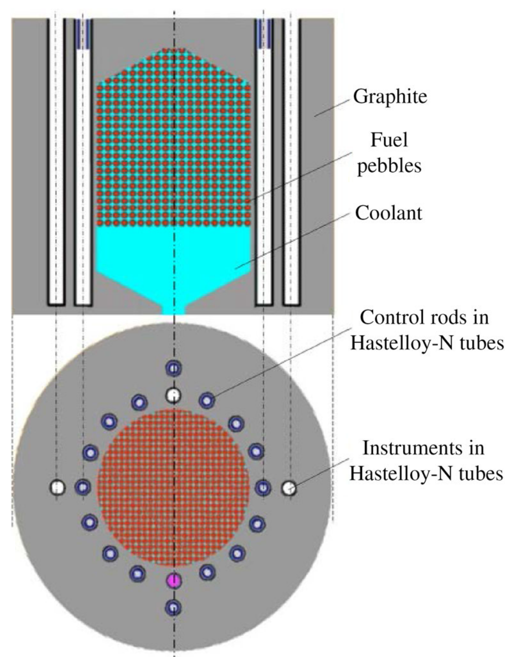

Fig. 1 The MCNP model for TMSR-SF1

3.1 The delayed fission neutron and photoneutron fraction

Using the k-ratio method described in Sect. 2.1, the delayed fission neutron and photoneutron fraction of TMSR-SF1 were simulated with 10^9 neutrons, as the (γ, n) reaction rate is very small. The critical eigenvalues were obtained with a statistical uncertainty of about 0.00003. The results are given in Table 2. The effectiveness fraction of the delayed fission neutron is about 1.04 in Mode N, while it is 0.27 for the ^{235}U fission [15]. The k-ratio method is very time-consuming for low statistical errors. Besides, photoneutrons generated in the active core and the reflector zones are of the same importance in the k-ratio method. Considering TMSR-SF1 has much more coolant in the reflector zone than in the active zone, the k-ratio method may overestimate the delayed photoneutron fraction.

3.2 Influence of photoneutrons on real time reactivity

The real time reactivity measurement, i.e., the reactivity meter, has been used widely [16, 17]. In this section, both positive and negative reactivity insertions are simulated. The theoretical basis is inverse point kinetics descried in Sect. 2.3.

3.2.1 Negative reactivity insertion

The largest impact of the photoneutrons is expected after shutdown of the reactor that has been operated at high power for a long time. According to the design of TMSR-SF1, the total worth of safety rods is about 6 \$ [6], and they should be fully inserted in 6 s at emergency. Such a scram was calculated. In the first 10 s, the reactor is operated at full power, then 6 \$ negative reactivity is fully inserted in 6 s.

The relative power level as a function of time following a scram from the full power is shown in Fig. 2a. In the calculation represented by "6 Group," the photoneutrons were not taken into account. Meanwhile, the one denoted by "15 Group," the photoneutrons were included in the calculation. The power difference between two cases grew gradually after shutdown. In the first 100 s, they did not differ from each other because the fission neutrons still took the major part. About 500 s latter, the presence of photoneutrons led to a 10 times larger power level. This can be explained by Eqs. (6–8). After shutdown, the number of photoneutrons was still determined by the original power, while the number of the fission neurons depended on the current low power. The relatively long decay time of relevant fission products made photoneutrons play an important role after shutdown.

The time-dependent reactivity calculated with and without considering photoneutrons is shown in Fig. 2b. In this simulation, the relative power obtained with photoneutrons is regarded as the truth (the blue line in Fig. 2a). One sees that, with photoneutrons, the reactivity meter gives great values, whereas it gives false values without photoneutrons. Although the reactor keeps subcritical after the scram, the reactivity meter without photoneutrons shows that positive reactivity is inserted gradually.

Table 2 Calculation of the effectiveness fractions for TMSR-SF1 by the k-ratio method

	β^{n} (pcm)	β^{ph} (pcm)
TMSR-SF1	679 ± 1.4	4 ± 1.4
^{235}U fission	650	15
Effectiveness fraction	1.04	0.27

3.2.2 Positive reactivity insertion

To evaluate the influence on positive reactivity, 0.1 \$ was inserted after full power operation for a long time. The power evolution after the positive reactivity insertion, shown in Fig. 3a, was simulated with and without the photoneutrons. It can be seen that the effect of delayed photoneutrons is similar to the delayed fission neutrons. The presence of photoneutrons slowed down the power increase. After 200 s of the reactivity insertion, "6 Group" power led to a power level of 10 times larger than the origin power, while the "15 Group" power led to a power level of 9 times larger than the origin level. The power evaluated with photoneutrons (blue line in Fig. 3a) was considered as the real case. The time-dependent reactivities calculated with and without the photoneutrons are shown in Fig. 3b. With photoneutrons, the reactivity meter met the truth, whereas the reactivity was overestimated when photoneutrons were neglected.

3.3 Influence of photoneutrons on doubling time measurement

The doubling time method is widely used for the control rod worth measurement, where the reactivity is calculated by the in-hour equation using the doubling time. The doubling time as a function of the positive reactivity inserted is shown in Fig. 4. In this calculation, follow the regulations, the doubling time was 30–180 s. As expected, the doubling time became longer for the same reactivity insertion by considering the photoneutron contribution. The 60 s doubling time corresponds to 0.108 \$ reactivity insertion for "6 Group," whereas to 0.112 \$ for "15 Group."

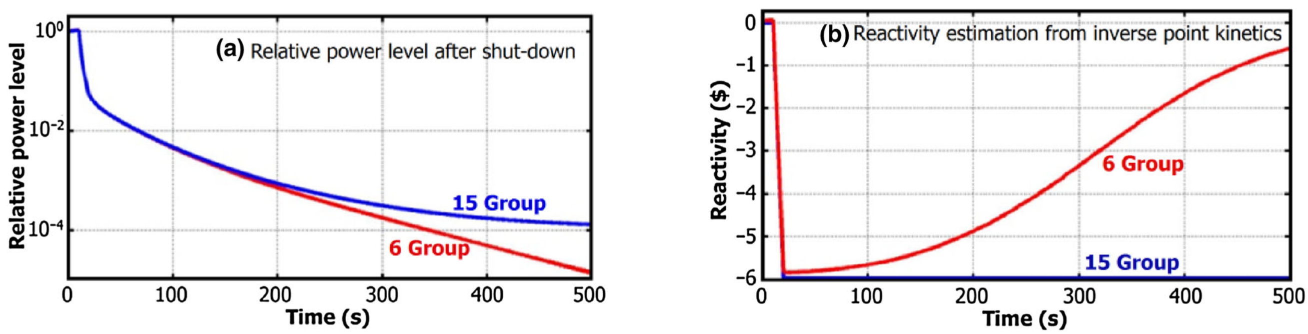

Fig. 2 Calculation of negative reactivity insertion (*15 Group* with photoneutrons; *6 Group* without photoneutrons)

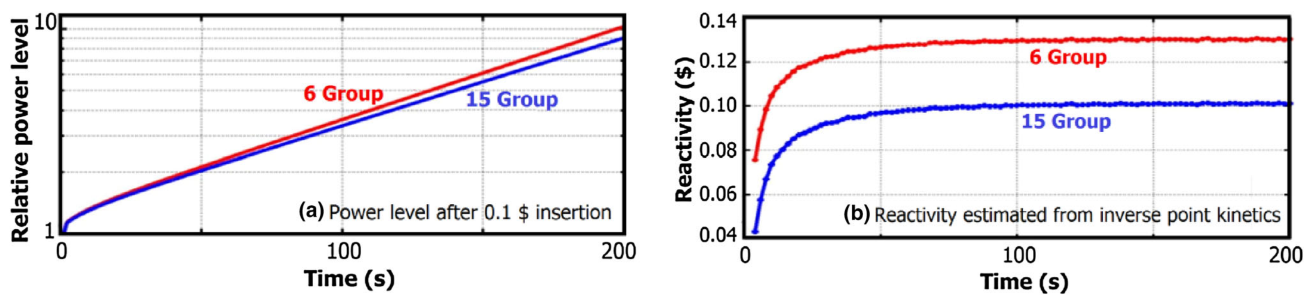

Fig. 3 Calculation of positive reactivity insertion (*15 Group* with the photoneutrons; *6 Group* without the photoneutrons)

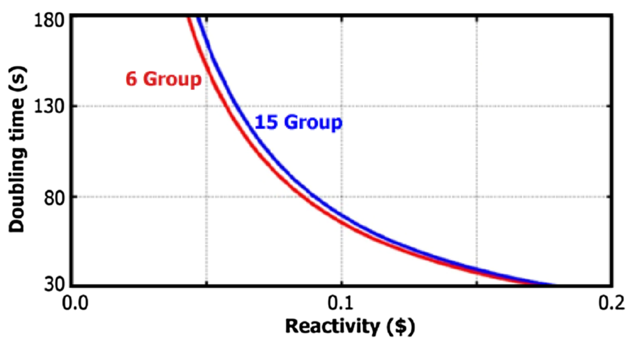

Fig. 4 Relationship between the doubling time and the positive reactivity inserted

In order to choose an appropriate waiting time before the reactivity measurement with respect to the positive reactivity insertion, calculations were carried out at different reactivities. The waiting time needed for 2% deviation from the doubling period is shown in Fig. 5a. The discrepancy in the waiting time was almost negligible for doubling periods close to 30 s, but became more apparent for longer doubling time. At 180 s of doubling time, the waiting time was less than 100 s for “6 Group,” but over 250 s for “15 Group.”

Since long-lived photoneutron precursors take extremely long time for saturation, it is not appropriate to always set the precursors’ concentrations as equilibrium condition. In this context, the building time is used to define the holding time at full power level before the shutdown step. The building time effect on the period measurement was calculated with 0.1 $ reactivity insertion. The error in doubling period measurement as the function of waiting time is shown in Fig. 5b. Obviously, much less waiting time is required in the non-equilibrium cases to reach the same accuracy as the equilibrium cases. When the reactor is at critical without external source, the equilibrium precursors to neutron flux is proportional to $1/\lambda_i$. The equilibrium precursors play an important role for the reactor of a positive period. The ones with non-equilibrium precursors have shorter asymptotic period. It increases more rapidly than the equilibrium case, so less waiting time is needed for the doubling period measurement.

3.4 Influence of photoneutrons on criticality estimation

Criticality measurements play an important role in reactor experiments. It is a usual method to bring the reactor to a steady power representing criticality. However, the limitation is that the effective multiplication factor, k_{eff}, equals to one only when the delayed neutron precursors have reached equilibrium. Since the delayed photoneutrons have much longer half-life than the delayed fission neutrons, it takes fairly long time to reach the equilibrium or decay from the equilibrium. Two conditions, non-saturated photoneutron precursors and extra precursors compared to the equilibrium, were analyzed.

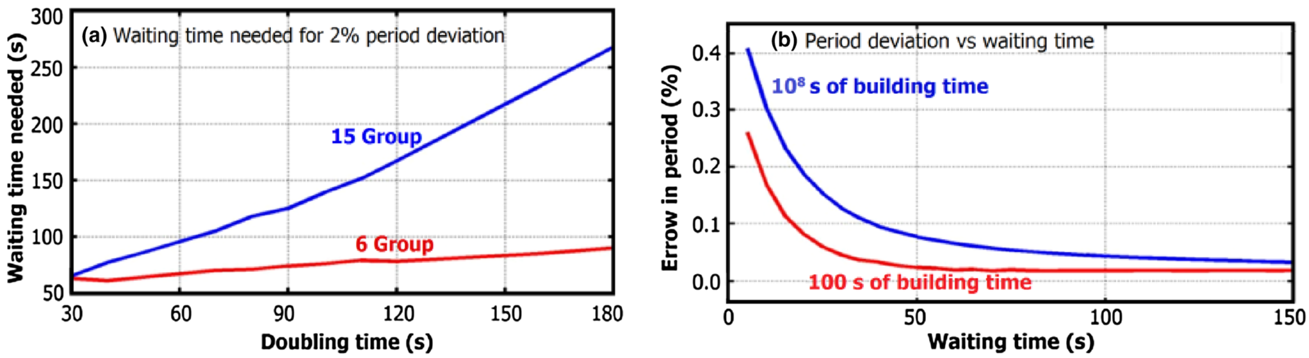

Fig. 5 Calculation of period deviation at 100 s and 10^8 s of building time, as a function of waiting time

3.4.1 *Non-saturation of the delayed photoneutron precursors*

With increasing precursors, more neutrons are being consumed than yielded when the power is steady. Thus, there is a net deficit in the neutron balance and some excess k_{eff} is required to keep the power steady. For math simplicity, it was assumed that the reactor was brought up to given power instantaneously and all precursors' concentrations were zero at the origin. Furthermore, the reactivity is constrained to maintain steady power, i.e., $dn/dt = 0$. A MATLAB code was written to find the root of Eqs. (6–8).

The excess k required to keep the power steady after start-up is shown in Fig. 6. In this calculation, different effectiveness factors were assumed. It can be predicted that the fission neutron precursors got equilibrium in 15 min while the photoneutron precursors did not reach equilibrium in 2 h. Hence, the reactor would need excess reactivity, about a few pcm, even after one or more hours. This may lead some trouble for high-precision measurements. As mentioned before, it was assumed that the reactor was brought up to steady power very rapidly, which is impossible in practice. So we made a correction for the finite start-up time by adding the time equal to the period that the reactor spent on bringing up the power. It should be emphasized that this effect applies only when the reactor is brought to power from shutdown. If the rector restores the steady power, the precursor equilibrium would be essentially undisturbed and no waiting time is needed for the criticality measurement.

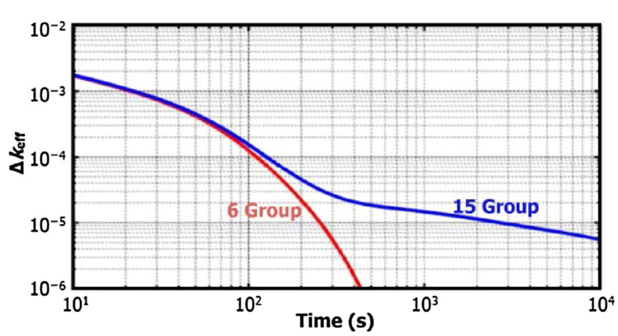

Fig. 6 Excess k required to hold steady power after start-up with and without the photoneutrons

3.4.2 *Extra photoneutron precursors compared to the equilibrium*

After operating at the high power level for a long time, the delayed photoneutrons originated from the fission products would decay slowly after the shutdown. As long as the delayed photoneutrons are strong enough, the reactor can restart without the external source which has been demonstrated in PIK reactor and MNSRs, where heavy water and beryllium are uses as the reflector [7, 18]. Similar to the last section, there is a net gain in the neutron balance and negative k_{eff} is required to keep the power steady when there are extra photoneutron precursors compared to the equilibrium.

4 Conclusion

In this work, we focused on addressing the impact of the photoneutrons in TMSR-SF1. The photoneutron contribution was calculated using k-ratio method by the MCNP5 code. Based on the coupled neutron–photon kinetics, the impact of the delayed photoneutrons was demonstrated in reactivity measurements. Conclusions drawn from this study are as follows:

(1) The result shows that the delayed fission neutron fraction in TMSR-SF1 is about 680 pcm, whereas the delayed photoneutron fraction is only 4 pcm. Although significant computational time was consumed to reduce the statistical uncertainty, the delayed photoneutron fraction obtained is not accurate.

(2) The presence of photoneutrons makes TMSR-SF1 more sluggish than the reactors without photoneutrons. The largest impact of photoneutrons can be found after the shutdown. The asymptotic period of the positive reactivity is greater than the case without photoneutrons. The critical extrapolation costs additional time due to the photoneutrons presence.

(3) Omitting photoneutrons in on-line reactivity measurement can lead to overestimation of the positive reactivity and underestimation of the negative reactivity.

(4) For the doubling time measurements, the presence of photoneutrons can increase the doubling time and the waiting time both. The increase in the waiting time is much more pronounced than that in the doubling time.

(5) Since the photoneutron precursors take very long time to reach equilibrium, the "steady" power operation may not directly imply a "real" criticality. If the precursors are unsaturated, the TMSR-SF1 needs slightly excessive reactivity to operate at steady power.

Since the delayed photoneutrons impact the reactivity measurement greatly for TMSR-SF1, the effectiveness of the photoneutrons will be further studied in the near future. Another reason is that the result calculated by the *k*-ratio method is not sufficiently accurate due to large statistical uncertainties.

Acknowledgements The authors thank Dr. Sun Kaichao for his careful revision of the manuscript.

References

1. T. Allen, S. Ball, E. Blandford, et al., Preliminary fluoride salt-cooled high temperature reactor (FHR) subsystems definition, functional requirement definition and licensing basis event (LBE) identification white paper. University of California, Berkeley, USA, UCBTH-12-001 (2012)
2. C. Forsberg, LW Hu, J Richard, et al., Fluoride-salt-cooled high temperature test reactor (FHTR): goals, options, ownership, requirements, design, licensing, and support facilities. Massachusetts Institute of Technology, USA, MIT-ANP-TR-154 (2014)
3. K. Sun, L. Hu, C. Forsberg, Neutronic design features of a transportable fluoride-salt-cooled high-temperature reactor. ASME J. Nucl. Rad. Sci. **2**, 031003-031003-10 (2016). doi:10.1115/1.4032873
4. D.F. Williams, L.M. Toth, K.T. Clarno, Assessment of candidate molten salt coolants for the advanced high-temperature reactor (AHTR). ORNL, USA, ORNL/TM-2006/12 (2006)
5. M.H. Jiang, H.J. Xu, Z.M. Dai, Advanced fission energy program—TMSR nuclear energy system. Bull. Chin. Acad. Sci. **27**, 366–374 (2012). doi:10.3969/j.issn.1000-3045.2012.03.016
6. TMSR group, TMSR-SF1 conceptual design overview, Chapter 2, Shanghai Institute of Applied Physics, Shanghai, China (2015)
7. I. Khamis, Evaluation of the photo-neutron source in the Syrian miniature neutron source reactor. Ann. Nucl. Energy **29**, 1365–1371 (2002). doi:10.1016/S0306-4549(01)00114-1
8. B. Dionne and N. Hanan. Impact of photoneutrons on transients for the MURR and MITR HEU and LEU cores, in *The 32nd RERTR 2010 International Meeting on Reduced Enrichment for Research and Test Reactors*, Lisbon, Portugal, 10–14 Oct 2010
9. C.E. Cohn, Errors in reactivity measurements due to photoneutron effects. Nucl. Sci. Eng. **6**, 284–287 (1959)
10. G. Hordósy, A. Keresztúri, P. Vértes, et al., Influence of the photoneutrons on the kinetics of the beryllium reflected core of the Budapest Research Reactor, in *Advanced Monte Carlo for Radiation Physics, Particle Transport Simulation and Applications*, Lisbon, Portugal, 23–26 Oct 2000
11. S.S. Lomakin, YuA Nechaev, Transient processes and the measurement of reactivity of a reactor containing beryllium. Sov. At. Energy **18**, 35–42 (1965). doi:10.1007/BF01116353
12. F.B. Buoni, Experience with the use of the rod-drop method of rod calibration at the ORR and LITR. ORNL, USA, ORNL-TM-605 (1963)
13. M.M. Bretscher, Perturbation independent methods for calculating research reactor kinetic parameters, Argonne National Laboratory, ANL/RERTR/TM30 (1997)
14. F. Jatuff, A. Lüthi, M. Murphy et al., Measurement and interpretation of delayed photoneutron effects in multizone criticals with partial D_2O moderation. Ann. Nucl. Energy **30**, 1731–1755 (2003). doi:10.1016/S0306-4549(03)00136-1
15. G.R. Keepin, *Physics of Nuclear Kinetics* (Addison-Wesley Publishing Company Inc., Boston, 1965)
16. W.F. Lv, F. Li, X.H. Zhou et al., Improvement and verification of inverse kinetics method. Nucl. Electron. Detect. Technol. **30**, 34–38 (2010). doi:10.3969/j.issn.0258-0934.2010.01.008. **(in Chinese)**
17. L.J. Meng, W. Lai, G.Q. Huang et al., Design and verification of a portable reactivity meter used for high temperature reactor. Nucl. Electron. Detect. Technol. **35**, 917–920 (2015). doi:10.3969/j.issn.0258-0934.2015.09.017. **(in Chinese)**
18. M.S. Onegin, Delayed photoneutrons in the PIK reactor. At. Energy **107**, 194–201 (2009). doi:10.1007/s10512-010-9215-1
19. Manuele Aufiero and Massimiliano Fratoni. Development of multi-physics tools for fluoride-cooled high-temperature reactors. PHYSOR 2016, Sun Valley, USA, 1–5 May 2016